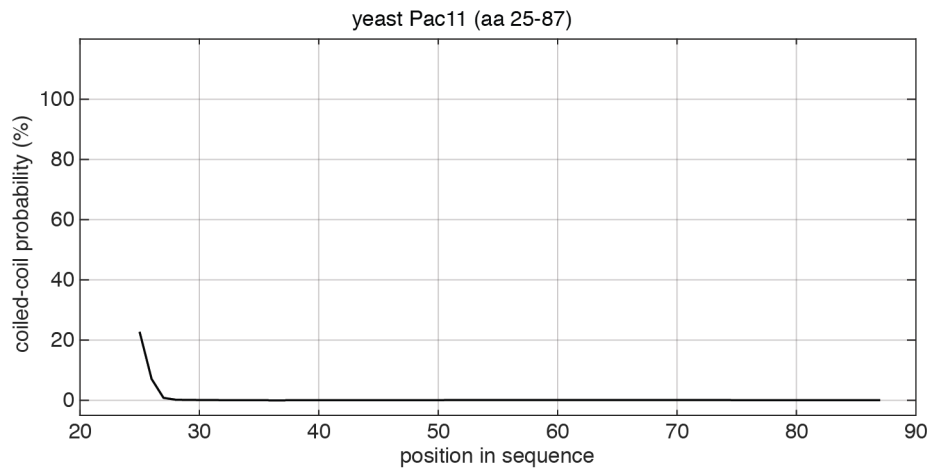
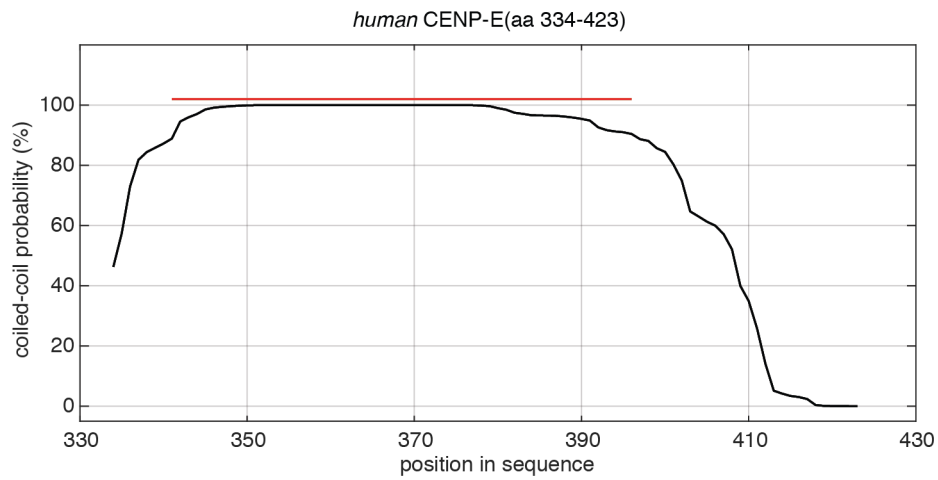
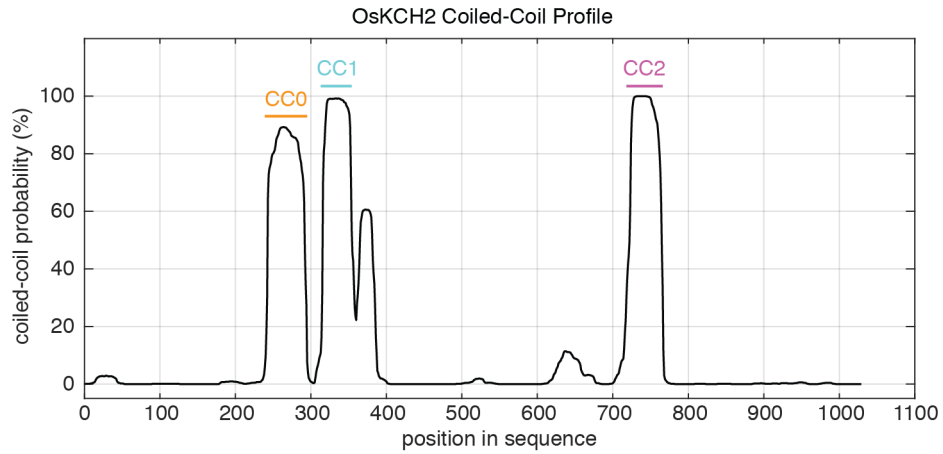


1

Supplementary Information

2

3 Supplementary Figures 1-8



4

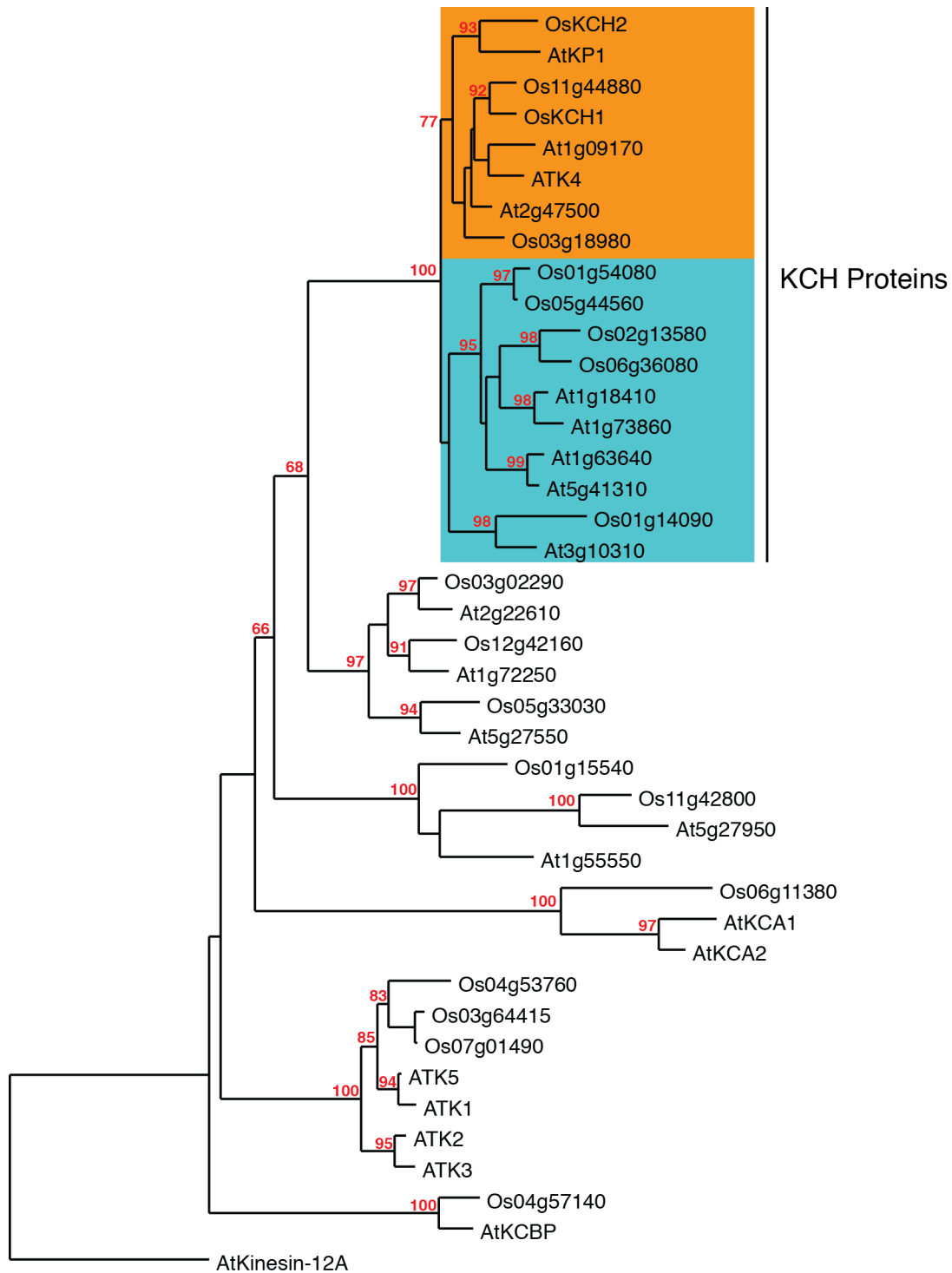
5 **Supplementary Figure 1: Predicted coiled-coil motifs of OsKCH2.** (Top) Based on
6 the prediction by the program MARCOIL with a coiled-coil cutoff probability of 80%, the
7 full-length OsKCH2 contains three coiled-coils, which include CC0 in aa 239-295, CC1
8 in aa 313-354, and CC2 in aa 718-766. (Middle) The predicted coiled-coil profile of
9 human kinesin-7 CENP-E(aa 343-423) by MARCOIL. Red line depicts the region that
10 forms an actual coiled-coil structure based on X-ray crystallography¹. This serves as a
11 positive control of the coiled-coil prediction of OsKCH2 by MARCOIL. (Bottom) The
12 predicted coiled-coil profile by MARCOIL of yeast Pac11(aa 25-87) that was
13 experimentally found to be intrinsically disordered². This serves as a negative control of
14 the coiled-coil prediction of OsKCH2 by MARCOIL³.

15
16

17

18

19



20

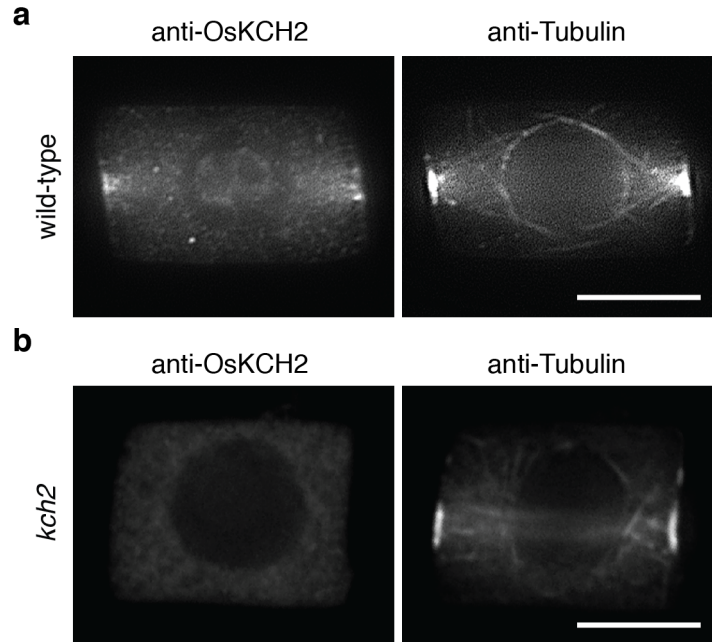
21 **Supplementary Figure 2: Phylogenetic tree of kinesin-14 motors from *Oryza***

22 ***sativa* and *Arabidopsis thaliana*.** The phylogenetic tree was generated with the

23 program PhyML (www.phylogeny.fr) based on the full-length protein sequences of the

24 kinesin-14 family from *Oryza sativa* (japonica cultivar) and *Arabidopsis thaliana*. The
25 maximum likelihood method was used. Branch support values were represented in
26 percentages (%), and only values greater than 60% were shown in the tree. Protein
27 sequence data of *O. sativa* (japonica cultivar) were obtained from MSU RGAP Release
28 7 (<http://rice.plantbiology.msu.edu/>; "LOC_" was omitted from each locus call) except for
29 OsKCH2, which was not annotated in the release; Protein sequence data of *A. thaliana*
30 were from TAIR10 (<http://www.arabidopsis.org/>); AtKCH1=LOC_Os12g36100.
31 AtKP1=At3g44730; ATK1=At4g21270/KATA; ATK2=At4g27180/KATB;
32 ATK3=At5g54670/KATC; ATK4=At5g27000/KATD; ATK5=At4g05190;
33 AtKCA1=At5g10470/KAC1; AtKCA2=At5g65460/KAC2; AtKCBP=At5g65930.
34 AtKinesin-12A/At4g14150 was included as an outgroup protein in the analysis.
35 Complete protein sequence alignment of all kinesin-14s in the phylogenetic tree can be
36 found in Supplementary Data 1.

37
38
39
40
41
42
43
44
45
46



47

48 **Supplementary Figure 3: OsKCH2 exhibits cortical localization in a rice cell at**
49 **prophase. a,** Immunostaining of a wildtype rice cell using anti-OsKCH2 (left) and anti-
50 Tubulin (right). **b,** Immunostaining of a *kch2* mutant cell using anti-OsKCH2 (left) and
51 anti-Tubulin (right). Scale bar: 5 μ m.

52

53

54

55

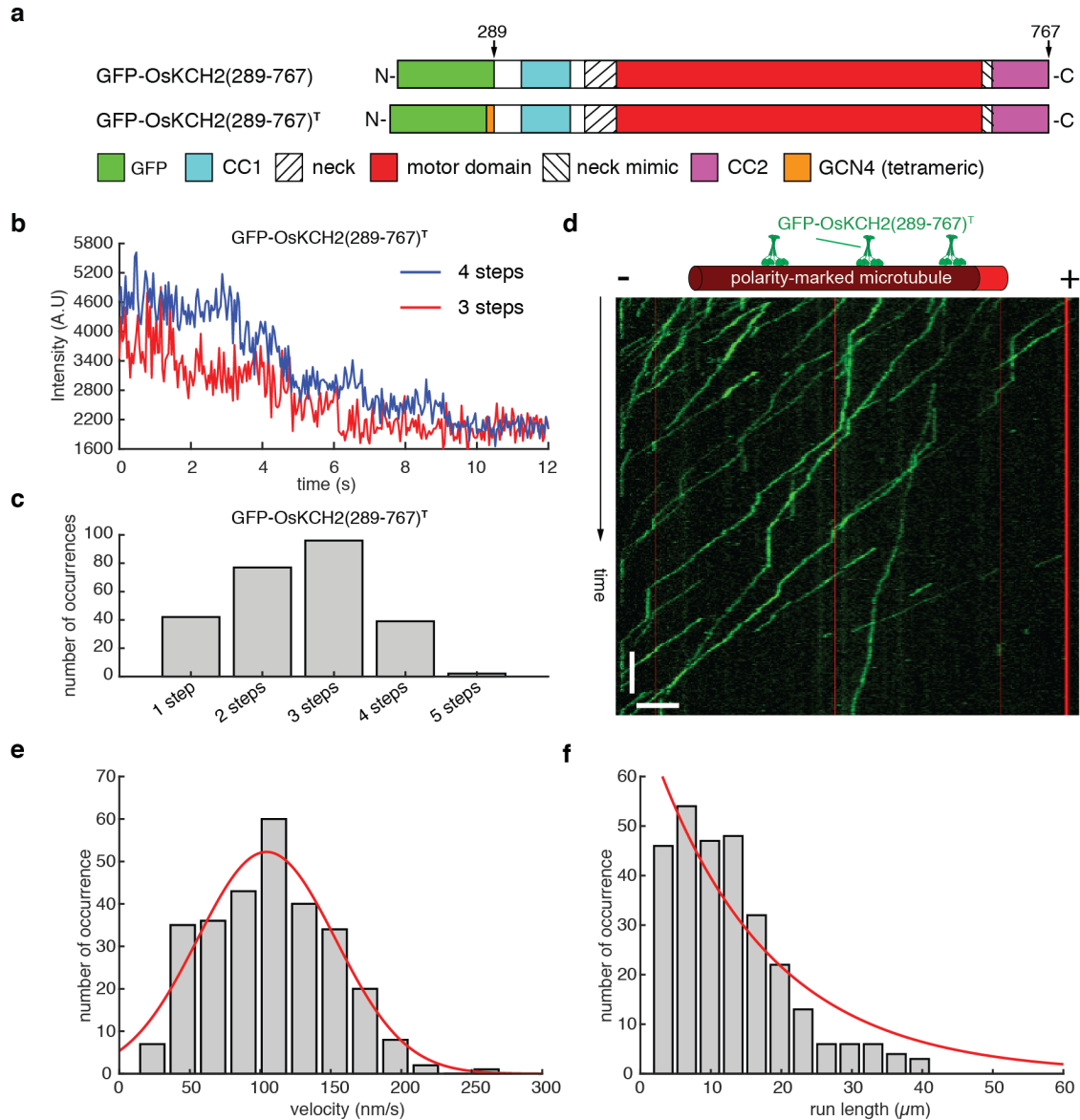
56

57

58

59

60



61

62 **Supplementary Figure 4: The artificial homotetramer GFP-OsKCH2(289-767)^T**

63 **exhibits ultraprocessive minus-end-directed motility on single microtubules. a,**

64 **Schematic diagrams of GFP-OsKCH2(289-767) and GFP-OsKCH2(289-767)^T. b,**

65 **Example fluorescence intensity traces over time of individual GFP-OsKCH2(289-767)^T**

66 **molecules immobilized on the microtubules. c, Histogram of the photobleaching steps of**

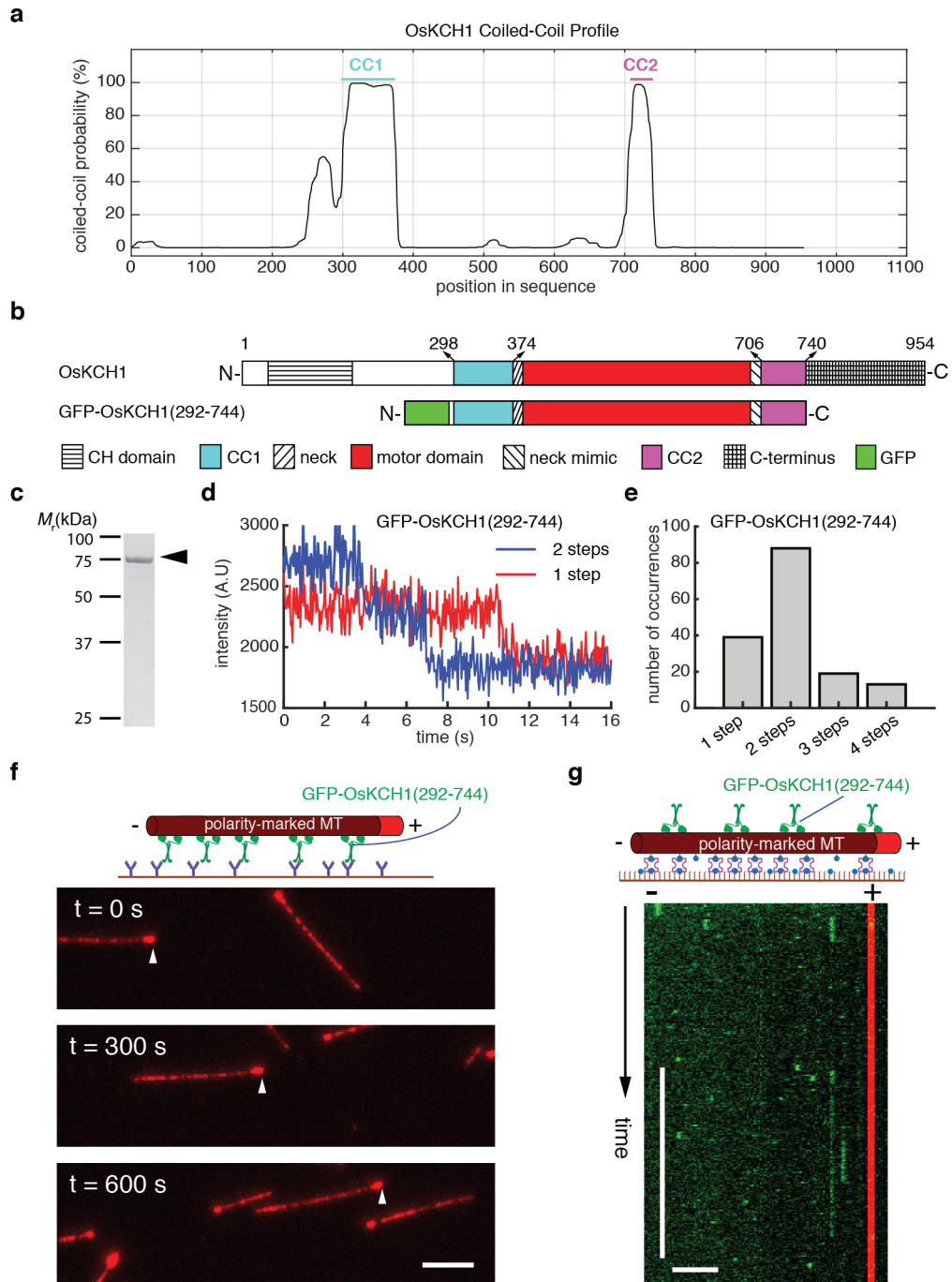
67 **GFP-OsKCH2(289-767)^T (n = 255). d, Example kymograph showing that individual**

68 **GFP-OsKCH2(289-767)^T molecules move processively toward the minus-end on a**

69 single microtubule. **e**, Velocity histogram of single GFP-OsKCH2(289-767)^T molecules.
70 Red line indicates a Gaussian fit to the velocity histogram. **f**, Run-length histogram of
71 single GFP-OsKCH2(289-767)^T molecules. Red line indicates a single-exponential fit to
72 the run-length histogram. Scale bars: 1 minute (vertical) and 5 μm (horizontal).

73

74



75

76

77

78

79 **Supplementary Figure 5: GFP-OsKCH1(292-744) is a nonprocessive minus-end-**
80 **directed microtubule motor. a,** Predicted coiled-coil motifs of OsKCH1. Based on the
81 prediction by the program MARCOIL with a coiled-coil cutoff probability of 80%. The full-
82 length OsKCH1 contains an upstream putative coiled-coil (CC1, aa 298-374) and a
83 downstream putative coiled-coil (CC2, aa 706-740). **b,** Schematic diagrams of the full-
84 length OsKCH1 and GFP-OsKCH1(292-744). **c,** Coomassie-stained SDS-PAGE of
85 purified recombinant GFP-OsKCH1(292-744). **d,** Example fluorescence intensity traces
86 over time of individual GFP-OsKCH1(292-744) molecules immobilized on the
87 microtubules. **e,** Histogram of the photobleaching steps of GFP-OsKCH1(292-744) (n =
88 156). **f,** Micrograph montage showing surface-immobilized GFP-OsKCH1(292-744)
89 molecules drive microtubules to glide with minus-end-directed motility. White
90 arrowheads indicate the plus ends of polarity-marked microtubules. **g,** Example
91 kymograph showing that individual GFP-OsKCH1(292-744) molecules are unable to
92 produce processive motility on a single microtubule. Scale bars: 30 s (vertical) and 5
93 μm (horizontal).

94

95

96

		10	20	30	40	50	60		
OsKCH2(289-767)	289	MKETSECF L T S L R L P C G R R K Q L D D G G G L E H Q Q E E L E K L K V S F N E M K L Q V E S T R S Q W E E D L R	349						
OsKCH1(292-744)	292	- - - - - G E V K Q F Q L E A Q T N F D V Q Q K Q I Q E L K G A L S F V K S G M E Q L R L Q Y S E E F A	338						
OsKCH2(289-767)	350	R L E S Y F E A H N - - H N A Y H K L L E E N R K L Y N Q V Q D L K G S I R V Y C R V K P F L K M Q T D Q R S T V D H I G	408						
OsKCH1(292-744)	339	K L G K H F Y T L S N A A S Y H K V L E E N R K L Y N Q I Q D L K G N I R V Y C R V R P F L P G H R S L S S V A D T E	399						
OsKCH2(289-767)	409	E N G E I M I V N P Q Q G K E G R K M F S F N K I F G P N A S Q S E V F A D T Q P L I R S V M D G Y N V C I F A Y G Q T	469						
OsKCH1(292-744)	400	E R - T I T I I T P T K Y G K D G C K S F S F N R V F G P A S T Q E E V F S D M Q P L I R S V L D G F N V C I F A Y G Q T	459						
OsKCH2(289-767)	470	G S G K T Y T M S G P D I T T E E T W G V N Y R S L N D L F A I S Q N R A D T T T Y D V K V Q M I E I Y N E Q V R D L L M	530						
OsKCH1(292-744)	460	G S G K T F T M S G P K V L T E E S L G V N Y R A L N D L F N I K A Q R K G T I D Y E I S V Q M I E I Y N E Q V R D L L Q	520						
OsKCH2(289-767)	531	V D G A N K R L E I R N S S H V N G L N I P D A N L V P V K C A Q D V L D L M R V G H R N R A V G S T A L N E R S S R S H	591						
OsKCH1(292-744)	521	- D G G N R R L E I R N T P O K - G L A V P D A S I V P V T S T A D V V E L M N Q G Q K N R A V G S T A I N D R S S R S H	579						
OsKCH2(289-767)	592	S V L T V H V Q G K E I A S G S T L R G C L H L V D L A G S E R V D K S E A A G E R L N E A K H I N K S L S A L G D V I A	652						
OsKCH1(292-744)	580	S C L S V H V Q G K Y L T S G A M L R G C M H L V D L A G S E R V D K S E V V G D R L K E A Q Y I N K S L S A L G D V I A	640						
OsKCH2(289-767)	653	A L A Q K S S H V P Y R N S K L T Q V L Q D A L G G Q A K T L M F V H M N P E A D A F G E T M S T L K F A E R V A T V E L	713						
OsKCH1(292-744)	641	S L A Q K N S H V P Y R N S K L T Q L L Q D S L G G Q A K T L M F V H V S P E L D A V G E T I S T L K F A E R V A S V E L	701						
OsKCH2(289-767)	714	G A A H A N K E V G Q V K D L K E E S K L K L A L D D K E R E A S K L R I A N R V A S E K R N A R T R S	767						
OsKCH1(292-744)	702	G A A K A N K G S E V R E L K S E I A T L K A A L A K K E G E P N I Q S T - - - - - - -	740						

97

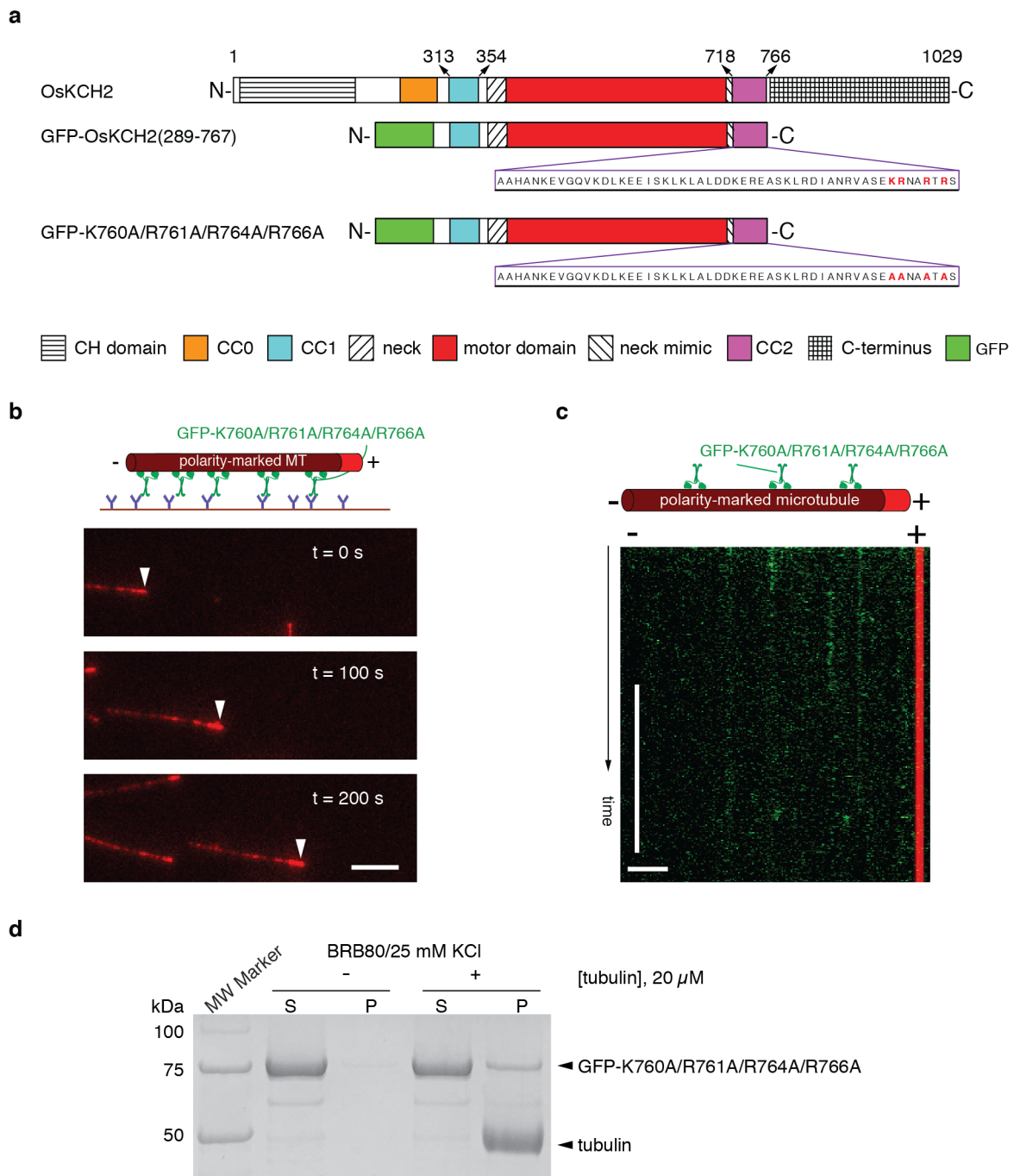
98 **Supplementary Figure 6: OsKCH2(289-767) and OsKCH1(292-744) differ**

99 **drastically in the CC2 region.** Pairwise protein alignment of OsKCH2(289-767) and

100 OsKCH1(292-744). The neck mimic region is indicated by asterisk (*) and the CC2

101 region is indicated by the underline. Positively charged residues in the CC2 region are

102 highlighted in blue and negatively charged residues in red.



103

104 **Supplementary Figure 7: The quadruple mutant GFP-K760A/R761A/R764A/R766A**

105 **is a nonprocessive minus-end-directed motor on single microtubules. a.**

106 Schematic diagrams of the full-length OsKCH2, GFP-OsKCH2(289-767) and GFP-

107 K760A/R761A/R764A/R766A. **b.** Micrograph montage showing that surface-immobilized
108 GFP-K760A/R761A/R764A/R766A molecules drive microtubules to glide with minus-
109 end-directed motility. White arrowheads indicate the plus ends of polarity-marked
110 microtubules. **c.** Example kymograph showing that individual GFP-
111 K760A/R761A/R764A/R766A molecules are unable to produce processive motility on a
112 single microtubule. **d.** Coomassie-stained SDS-PAGE of the microtubule co-
113 sedimentation assay for GFP-K760A/R761A/R764A/R766A in BRB80/25 mM KCl.
114 Scale bars: 30 s (vertical) and 5 μ m (horizontal).

115

116

117

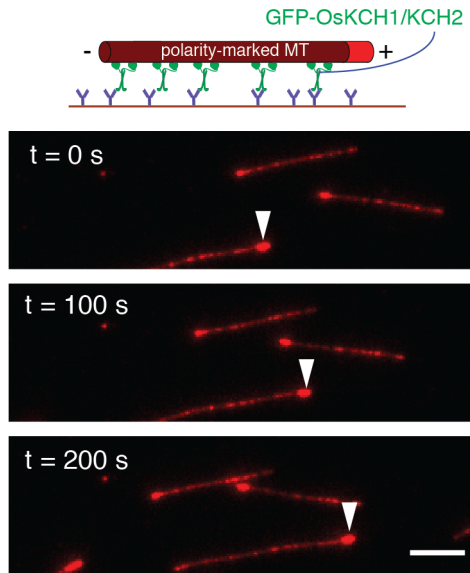
118

119

120

121

122



123

124 **Supplementary Figure 8: GFP-OsKCH1/KCH2 exhibits minus-end-directed motility**

125 **in the ensemble microtubule-gliding assay.** Micrograph montage showing surface-

126 immobilized GFP-OsKCH1/KCH2 molecules drive microtubules to glide with minus-end-

127 directed motility. White arrowheads indicate the plus ends of polarity-marked

128 microtubules.

129

130 **Supplementary References:**

131

- 132 1. Phillips, R. K., Peter, L. G., Gilbert, S. P. & Rayment, I. Family-specific kinesin
133 structures reveal neck-linker length based on Initiation of the coiled-coil. *J. Biol.*
134 *Chem.* **291**, 20372–20386 (2016).
- 135 2. Jie, J., Löhr, F. & Barbar, E. Interactions of yeast dynein with dynein light chain and
136 dynactin: General implications for intrinsically disordered duplex scaffolds in
137 multiprotein assemblies. *J. Biol. Chem.* **290**, 23863–23874 (2015).
- 138 3. Delorenzi, M. & Speed, T. An HMM model for coiled-coil domains and a
139 comparison with PSSM-based predictions. *Bioinformatics* **18**, 617–625 (2002).

140